Study of the Elementary Processes Involved in the Selective Oxidation of Methane over MoO_x/SiO_2

Nicholas Ohler and Alexis T. Bell*

Department of Chemical Engineering, University of California, Berkeley, California 94720-1462

Received: August 16, 2005

Isolated molybdate species supported on silica are reported to have the highest specific activity and selectivity for the direct oxidation of methane to formaldehyde. The present investigation was undertaken to understand the elementary redox processes involved in the formation of formaldehyde over such species. A MoO_x/SiO_2 catalyst was prepared with a Mo loading of 0.44 Mo/nm^2. On the basis of evidence from extended X-ray absorption fine structure (EXAFS) and Raman spectroscopy, the Mo atoms in this catalyst are present as isolated, pentacoordinated molybdate species containing a single Mo═O bond. Isotopic labeling experiments in combination with in-situ Raman spectroscopy were used to examine the reducibility of the dispersed molybdate species and the exchange of O atoms between the gas phase and the catalyst. It was established that treatment of MoO_x/SiO_2 at 873 K under pure methane reduces the dispersed molybdate species to only a limited extent and results mainly in the deposition of amorphous carbon. During CH_4 oxidation to formaldehyde, the catalyst undergoes only a very small degree of reduction and typically only ∼50−500 ppm of Mo^{VI} is reduced to Mo^{IV}. Reactions carried out using CH_4 and $^{18}O_2$ show that there is extensive scrambling of O atoms between the species in the gas phase and the catalyst. Additional experiments revealed that H_2O formed in the reaction is the principal species responsible for the exchange of O atoms between the gas phase and the SiO_2 support. Low concentrations of H_2O were observed to enhance the activity of MoO_x/SiO_2 for CH_4 oxidation to formaldehyde. A mechanism for the oxidation of CH_4 over MoO_x/SiO_2 was formulated in light of the observations made here and is discussed in the light of previous studies. It is proposed that peroxides are produced by the reaction of O_2 with a small concentration of reduced molybdate species and that the reaction of CH_4 with these peroxide species leads to the formation of formaldehyde. The proposed mechanism also accounts for the positive effects of low concentrations of H_2O on the rate of formaldehyde formation.

Introduction

The direct oxidation of methane to formaldehyde in a single step is a potentially attractive process for upgrading natural gas to a more valuable chemical feedstock. Such a process could in principle become competitive with the indirect conversion of methane to formaldehyde, which involves three separate steps—steam reforming of methane to produce synthesis gas, conversion of synthesis gas to methanol, and partial oxidation of methanol to formaldehyde. While highly dispersed MoO_x and VO_x supported on SiO_2 are known to be active for the direct oxidation of methane to formaldehyde, the highest single-pass yields of formaldehyde are typically on the order of 2−5%.[1−5] As a result, there is considerable interest in understanding the elementary processes involved in the formation and loss of formaldehyde, so that this knowledge might be used to prepare more highly selective catalysts.

The reaction mechanism for the conversion of methane to formaldehyde over SiO_2-supported MoO_x has been investigated by a number of authors, and several schemes have been proposed to explain the kinetics of methane oxidation to formaldehyde and spectroscopic observations of the catalyst.[1,6−10] A common feature in these schemes is the involvement of multiple Mo centers in one or more of the elementary steps involved in transforming methane to formaldehyde. While effective in describing the observed reaction kinetics, the inclusion of such elementary steps fails to explain why the highest specific activity for MoO_x/SiO_2 occurs at Mo surface concentrations of <1 Mo/nm^2, for which virtually all of the Mo is present as isolated molybdate species.[11−20] Since gas-phase free-radical reactions are insignificant during methane oxidation over MoO_x/SiO_2,[1,21] it is not clear how multiple isolated molybdate centers are able to participate in the oxidation of methane and the reduction of molecular oxygen. Observations made during experiments involving 18-labeled oxygen and during experiments in which H_2O is added to the feed give rise to further questions regarding the reaction mechanism. Isotopic labeling experiments have revealed that oxygen from the SiO_2 support is incorporated extensively into the oxygenated products of methane oxidation formed over SiO_2-supported MoO_x and VO_x,[22,23] suggesting that labile SiO_2 oxygen may be involved in the oxidation of CH_4. Both a positive and a negative influence of H_2O on the rate of CH_4 oxidation has been reported for oxidation of CH_4 by O_2,[10,24−26] but a mechanism has not been proposed to explain the chemical effect of H_2O on the reaction.

The aim of the present work was to understand the elementary processes involved in the oxidation of CH_4 over a MoO_x/SiO_2 catalyst in which the Mo is present solely as isolated molybdate species. X-ray absorption spectroscopy (XAS) and O_2 titration were used to determine the oxidation state of Mo after reduction

* To whom correspondence should be addressed. E-mail: bell@cchem.berkeley.edu.

10.1021/jp058229u CCC: $33.50
Published on Web 01/26/2006

by CH_4, CH_2O, CO, and H_2. XAS was also used to monitor the oxidation state of Mo during steady-state oxidation of CH_4, and O_2 titration was used to determine the number of reduced centers during reaction. Raman spectroscopy and mass spectrometry were used simultaneously during CH_4 oxidation by $^{18}O_2$ and during exchange of oxygen between $H_2{}^{18}O$ and MoO_x/SiO_2 in order to investigate the transfer of oxygen between the gas phase and the catalyst during CH_4 oxidation. The effect of the H_2O partial pressure on the rate of CH_4 oxidation was determined by varying the H_2O and CH_4 feed fractions during CH_4 oxidation. A reaction mechanism is formulated based on the experimental results gathered here and is assessed in light of previous work.

Experimental Section

Sample Preparation. Silica gel (Silicycle R10070B-00, 60 Å pore diameter) was washed in 9 M HNO_3 at 333 K, rinsed thoroughly with deionized water, and calcined in flowing air for 3 h at 973 K in order to remove alkaline earth impurities.[8,27] This treatment reduced the silica surface area from 500 m^2/g to 460 m^2/g, as measured by five-point analysis of the BET adsorption isotherm. MoO_x/SiO_2 was prepared by impregnation with an aqueous solution of ammonium heptamolybdate (AHM) tetrahydrate (Aldrich, 99.98% pure). AHM (0.067 g) was suspended in 2.1 g of deionized water (150% of the pore-filling amount) for each gram of silica gel to be impregnated. The expected Mo loading was thus 3.5 wt % elemental Mo. The suspension was immersed in a bath heated at 333 K and stirred until the solvent was evaporated. The resulting solid was oven dried at 383 K overnight and calcined under flowing air at 873 K for 3 h. The surface area of the calcined catalyst was 426 m^2/g. The Mo weight fraction determined by elemental analysis (Galbraith Laboratories) was 3.0% (4.5 wt % as MoO_3), so that the nominal surface coverage of MoO_x was 0.44 Mo/nm^2.

Characterization of MoO_x/SiO_2 by X-ray Absorption Spectroscopy. The procedures used for the collection of X-ray absorption spectra at the Mo K-edge have been described previously.[28] XAS was performed at the Stanford Synchrotron Radiation Laboratory (SSRL) on beamline 2−3 using an Si(220) monochromator. MoO_x/SiO_2 samples were pretreated by heating at 10 K/min to 873 K in flowing 10% O_2/He, holding at 873 K for 2 h, and then cooling to room temperature, after which the sample was evacuated to a residual pressure of $\sim 10^{-5}$ Torr. The cell was then repressurized with CH_4 (Praxair UHP), 4% CO/He (Matheson certified standard), or H_2 (Praxair UHP), and the sample was heated under continuous gas flow at 10 K/min to 873 K. Spectra were recorded at 873 K and were subsequently recorded in vacuo at 77 K. To investigate catalyst reduction by CH_2O, the evacuated cell was heated to 473 K before introducing a flow of ~1% CH_2O/He, which was generated by flowing He (Matheson UHP) through a saturator filled with beads of solid paraformaldehyde (Aldrich, 95% pure). The saturator temperature was maintained at 331 K by recirculating heated water through a heating jacket surrounding the saturator. A Thermo Electron Neslab RTE-7 recirculating heater/chiller was used to maintain the saturator temperature. Observations of the edge energy of MoO_x/SiO_2 under He following air calcination and under a feed of 90% CH_4/10% O_2 were made in a separate set of experiments carried out at Brookhaven National Laboratory. The energy resolution for these measurements was poorer than for those performed at SSRL because an Si(111) monochromator was used. The areas of the pre-edge features from this set of experiments could not be compared with those gathered at higher resolution, but the edge energies could be determined by comparison with the spectrum observed in flowing 10% O_2/He gathered in the same set of experiments.

Extended X-ray absorption fine structure (EXAFS) data were analyzed with the Athena XAS software analysis package.[28] Spectra were gathered in triplicate, aligned using the edge energy measured simultaneously for Mo foil, normalized by fitting cubic splines over the pre-edge region from −150 to −75 eV and over the postedge region from 0.5 to 16.0 $Å^{-1}$, and then averaged. The Autobk method was used to remove background absorption Fourier components for $R < 1.0$ Å using a k^3-weighted transform ($R_{bkg} = 1.0$ Å) in order to obtain the EXAFS function $\chi(k)$. The k^3-weighted transform of $\chi(k)$ was obtained over the region $2.5 < k < 13.2$ $Å^{-1}$ using a Kaiser−Bessel window.

O_2 Titration of Reduced MoO_x/SiO_2. O_2 pulse chemisorption was performed at 873 K according to established procedures.[30] For samples treated under pure CH_4 and pure H_2, the thermal conductivity detector of an Agilent 6890 N gas chromatograph was used to detect O_2 not adsorbed by the samples. Data points were gathered at a frequency of 5 Hz. For samples treated under CH_4/O_2 mixtures, the amount of O_2 chemisorption was much smaller and an MKS Minilab mass spectrometer was utilized to detect O_2 not adsorbed by the samples. A high sampling rate of ~5 Hz was achieved with an accuracy setting of 8 (2^8 measurements per sample) by putting the spectrometer in "peak jump" mode and measuring only $m/e = 32$ without recalibrating m/e between scans.

Sample masses of ~100 mg were used for treatment in pure CH_4 or H_2 and of ~500 mg for samples treated in CH_4/O_2 mixtures. Calcined samples were loaded into a quartz microreactor,[1] heated at 10 K/min to 873 K and held for 30 min, purged in pure He (Praxair UHP) for 15 min, and then exposed to pure CH_4 (Matheson research grade), pure H_2 (Praxair UHP), or a mixture of CH_4 and O_2 (Matheson UHP) for 30 min. After treatment, the sample was purged in He until the detector signal reached the baseline (~20 min for the TCD or ~3 min for the MS). Gas flow rates were maintained at 30 cm^3(STP)/min during treatment under CH_4 or H_2 and at 60 cm^3(STP)/min during treatment under CH_4/O_2 mixtures. During treatment under CH_4/O_2 mixtures, the reactor effluent was monitored with the mass spectrometer, to ensure that oxygen conversion was incomplete. Oxygen conversion was at most ~ 70%. Four-way switching valves (Swagelok 40 series) were used to switch between gas flows. Square pulses of O_2/He were introduced at room temperature into the He stream using a six-way crossover valve (Swagelok 40 series). A 0.421 cm^3 sample loop was used to set the pulse size. For CH_4- and H_2-treated samples, 10.3% O_2/He (Matheson certified standard) was used to generate pulses containing 1.79 μmol O_2. For samples treated in CH_4/O_2 mixtures, 1000 ppm O_2/He (Praxair certified standard) was used to generate pulses containing 17.4 nmol O_2. Pulses were injected into the He stream at 2 min intervals for CH_4- and H_2-treated samples or at 40 s intervals for samples treated in CH_4/O_2. Pulses were injected until the detected area was constant for at least three consecutive pulses. The oxygen uptake was calculated from the following equation

$$n_O^{sample} = 2 \times n_{O_2}^{loop} \left(\frac{N \times A_f - \sum_{i=1}^{N} A_i}{A_f} \right)$$

where n_O^{sample} is the moles of O adsorbed by the sample, $n_{O_2}^{loop}$ is the moles of O_2 contained in a full pulse, N is the total number

of pulses injected, A_i is the detected area of the ith pulse, and A_f is the area of the final pulse, corresponding to a full pulse. Chemisorption of O_2 by the H_2-reduced empty reactor was small but measurable (~0.5 μmol O), and this amount was subtracted from the amount adsorbed by H_2-reduced MoO_x/SiO_2 samples, which was on the order of 36 μmol O. No O_2 chemisorption was measurable for H_2-reduced SiO_2, and no O_2 chemisorption was measurable for the empty reactor or for bare SiO_2 treated in pure CH_4 or CH_4/O_2 mixtures.

Characterization of MoO_x/SiO_2 by Raman Spectroscopy. A heated quartz microreactor containing a rotating sample holder was used for the acquisition of in-situ Raman spectra. A detailed description of this apparatus has been presented previously.[28,31] Sample masses were typically 31 mg. He (Praxair UHP), CH_4 (Matheson research grade), 10.3% O_2/He (Matheson certified standard), and 20% $^{18}O_2$/He (Isotec, >99% O_2 isotopic purity) were metered into the cell using Porter 201 mass flow controllers. The mass flow controllers were calibrated at multiple points with a soap bubble meter. Flow setpoints were applied manually using a Porter PCIM-4 control unit. $H_2{}^{18}O$ was introduced into the He stream by directing the flow through a 15 mL gas-washing bottle (LabGlass ML-1490-710) filled with $H_2{}^{18}O$ (Isotec/Sigma-Aldrich, >95% O isotopic purity) at room temperature and with 1 mm glass beads (Cole-Parmer 36270-50) to raise the liquid level. All tubing and valves located downstream of the gas-washing bottle were maintained at ~333 K to prevent condensation. Total gas flow rates were 20 or 31 cm^3(STP)/min. The heated volume of the Raman cell was estimated to be 15 cm^3. Four-way crossover valves (Swagelok 40 series) were used to switch between gas flows.

Deconvolution of the Raman spectra of SiO_2 and MoO_x/SiO_2 was carried out using the procedure described in ref 28. Only the essential aspects of the procedure are summarized here. The spectra of MoO_x/SiO_2 were fit by summing the Lorentzian components for each of the Raman-active SiO_2 and MoO_x features including the SiO_2 D_2 feature and the Mo=O stretching vibration, observed at 614 and 988 cm^{-1}, respectively, for $^{16}O_2$-calcined MoO_x/SiO_2.[13,32,33] During ^{18}O exchange, the Mo=^{16}O band at 988 cm^{-1} decreased in intensity and a separate Mo=^{18}O band appeared at 938 cm^{-1}, which increased in intensity. The fraction of the molybdenyl occupied by ^{16}O was calculated from the fraction of the total Mo=O area in the 938 cm^{-1} peak

$$\frac{A_{938}}{A_{938} + A_{988}}$$

The D_2 feature of SiO_2 has been attributed to either cyclic $(Si-O-)_3$ moieties[32,34,35] or homopolar Si−Si and O−O bonds at the SiO_2 surface.[36,37] This band is well-resolved and is red shifted by 33 cm^{-1} as the ^{16}O in the feature is replaced with ^{18}O. Therefore, the position of the D_2 band is a useful measure of the isotopic composition of the oxygen of the SiO_2 surface. It was assumed that the position of the D_2 peak is linearly proportional to the fraction of ^{18}O-labeled oxygen incorporated into the structure responsible for the band. Therefore, the fraction of ^{16}O in the feature was calculated as the accomplished change in the peak position

$$\frac{\mu_{D2} - \mu_{D2}{}^{18}}{\mu_{D2}{}^{16} - \mu_{D2}{}^{18}}$$

μ_{D2} is the peak position of the D_2 feature, and $\mu_{D_2}{}^{16}$ and $\mu_{D_2}{}^{18}$ are the peak positions of the D_2 feature with pure ^{16}O and pure ^{18}O, respectively.

Analysis of Gas-Phase Composition during Isotope Exchange Experiments. Isotopic exchange experiments were carried out to determine the rate at which gas-phase $H_2{}^{18}O$ exchanges O atoms in the catalyst and the rate at which ^{18}O is incorporated into the catalyst during CH_4 oxidation by $^{18}O_2$. These experiments were carried out in the Raman cell. The isotopic composition of the effluent from the Raman cell was monitored with an MKS Minilab mass spectrometer. Data were gathered in analogue mode using 16 points per mass, sweeping from $m/e = 1$ to 50. An accuracy setting of 5 was used (2^5 samples per data point), allowing the collection of 1 mass spectrum every 41 s. Peak maxima were used for quantification of partial pressures. Response factors were determined relative to He for all of the fragments of CH_4, CH_2O, CO, CO_2, H_2, O_2, and H_2O by multipoint calibration, and the appropriate corrections were made to the fragmentation patterns of O_2 and H_2O to account for the natural abundance of ^{18}O. It was assumed that the response factors for ^{18}O-containing fragments were identical to those of the corresponding ^{16}O-containing fragments. CH_4 produced fragments from $m/e = 26$ to $m/e = 30$ from fragment combination that interfered with the peaks of CH_2O and CO and that were second order with respect to CH_4 partial pressure. The apparent linear response factors of these fragments were determined from a single-point calibration at the molar fraction of CH_4 employed in the feed in this study (40%). The relative response factors at $m/e = 2$, 12−16, 18, 20, 27−36, and 44−49 for the oxygen isotopomers of each of the components were assembled into a matrix. The Moore−Penrose inverse of this matrix was applied to each vector of relative intensities of the listed mass fragments to yield each composition vector including all of the oxygen isotopes.

Measurement of Catalytic Activity. Catalytic activity was measured using the flow reactor described previously.[1] An amount of 196 mg of 0.44 Mo/nm^2 MoO_x/SiO_2 was supported on quartz wool in a quartz tube (6 mm ID) and was heated to 873 K at 10 K/min in flowing air prior to the introduction of reactants. CH_4 (Matheson research grade), O_2 (Matheson UHP), and He (Praxair UHP) were metered into the flow manifold by Porter 201 mass flow controllers. H_2O was introduced into the He stream by directing the flow through a 15 mL gas-washing bottle (LabGlass ML-1490−710) filled with deionized H_2O. The gas-washing bottle was immersed in a bath. The H_2O feed fraction was varied by adjusting the temperature of the bath, which was controlled by a Thermo Electron Neslab RTE-9 recirculating heater/chiller. An HP 6890 N gas chromatograph equipped with a heated 250 μL sampling loop was used to measure the composition of both the reactor feed and the reactor effluent. A 30 foot long, 1/8 in. diameter column packed with Hayesep DB 80/100 mesh was used to separate all components. The column temperature was held at 278 K for 7 min, ramped at 45 K/min to 423 K, and held at 423 K for 15 min. Eluted components were detected with a thermal conductivity detector.

Results and Discussion

Catalyst Structure. We have recently described the structural characterization of the MoO_x/SiO_2 sample utilized in this work by Raman spectroscopy and XAS.[28] The magnitude of the k^3-weighted Fourier transform of the $\chi(k)$ EXAFS spectrum of the sample contained no backscattering peaks in the range from 2.5 to 4.0 Å characteristic of Mo−Mo backscattering, demonstrating that the MoO_x are isolated from each other on the SiO_2 surface. The edge energy of the calcined MoO_x/SiO_2 was consistent with assignment of the oxidation state as Mo^{VI}. The area of the pre-edge feature in the XANES region was similar

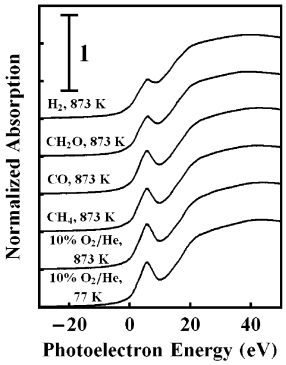

Figure 1. Normalized XANES spectrum of MoO_x/SiO_2 recorded in vacuo at 77 K following calcination in 10% O_2/He and recorded in-situ at 873 K under flowing 10% O_2/He, pure CH_4, 4% CO/He, 1% CH_2O/He, and pure H_2.

TABLE 1: Shift in Mo K-Edge Energy Relative to Mo Foil and Integrated Area of the Pre-edge Peak for MoO_x/SiO_2 at 873 K under Various Flowing Gases

gas	edge energy (eV)	area of pre-edge peak (eV)
10% O_2/He	8.1	2.2
He	8.1	*a*
90% CH_4/10% O_2	7.9	*a*
CH_4	7.8	1.9
4% CO/He	7.6	1.9
1% CH_2O/He	6.2	1.3
H_2	5.0	0.96

[a] Spectra recorded at lower resolution and aligned with spectrum gathered in flowing air at similar resolution; pre-edge peak areas not comparable to those observed at higher resolution.

in intensity to that of $(NH_4)_2Mo_2O_7$, which contains octahedrally coordinated and tetrahedrally coordinated Mo in a 1:1 ratio.[38] Such a pre-edge feature area is expected for pentacoordinate MoO_x. The Raman spectrum exhibits only a single Mo═O stretch, or two Mo═O stretches upon partial replacement of Mo═^{16}O with Mo═^{18}O, indicating that the supported MoO_x has only a single terminal oxo group.[39,40] The SiO_2-supported MoO_x species are therefore isolated, pentacoordinated, $Mo^{VI}O_x$ moieties containing a single terminal oxo (Mo═O) function. This assignment is in agreement with previous studies.[11−20,39−41]

Reducibility of MoO_x/SiO_2. The reducibility of MoO_x/SiO_2 by CH_4 and by the products of CH_4 oxidation was investigated by in-situ XAS. Mo K-edge XANES spectra of MoO_x/SiO_2 taken during catalyst reduction with CH_4, CH_2O, CO, and H_2 at 873 K are shown in Figure 1. For reference, XANES spectra of fully oxidized MoO_x/SiO_2 taken in flowing O_2/He at 873 K and in a vacuum at 77 K are also shown. Edge energies were determined for each of the samples relative to Mo foil. This was done by aligning the rising slopes of the spectra in the region of 20 010−20 020 eV. The edge energy relative to Mo foil (20 000 eV) and the integrated intensity of the pre-edge feature are listed in Table 1 for each sample. The edge energy observed under flowing He following calcination was identical to that observed under flowing 10% O_2/He, demonstrating that MoO_x/SiO_2 does not undergo autoreduction at 873 K. In pure CH_4, the edge energy was 7.8 eV, a shift of only −0.3 eV relative to the energy of fully oxidized MoO_x/SiO_2, and the integrated intensity of the pre-edge feature decreased from 2.2 to 1.9 eV. Under 4% CO/He, an edge energy of 7.6 eV was observed and the integrated intensity of the pre-edge feature was identical to that observed during reduction by CH_4. These results suggest that neither CH_4 nor CO are capable of reducing MoO_x/SiO_2 significantly at 873 K. The edge energy decreased

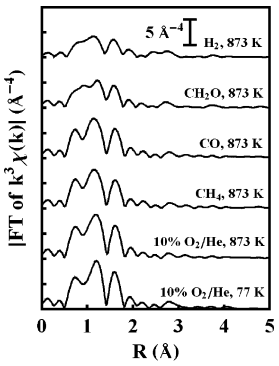

Figure 2. Magnitude of k^3-weighted Fourier transform of $\chi(k)$ for calcined MoO_x/SiO_2 at 77 K recorded in vacuo following calcination in 10% O_2/He and recorded in-situ at 873 K under flowing 10% O_2/He, pure CH_4, 4% CO/He, 1% CH_2O/He, and pure H_2. Not corrected for phase shift.

to 6.2 eV during reduction in 1% CH_2O and the integrated intensity of the pre-edge feature decreased to 1.3 eV. An even greater decrease in the edge energy and the integrated intensity of the pre-edge feature was observed for reduction in H_2. In this case, the edge energy decreased to 5.0 eV and the integrated intensity of the pre-edge feature decreased to 0.96 eV. When a mixture of 90% CH_4/10% O_2 was passed over the catalyst at 873 K, the Mo K-edge shifted to 7.9 eV, only 0.2 eV lower than that observed for the fully oxidized catalyst.

On the basis of our study of MoO_x/SiO_2 reduction by H_2 at 873 K, using the same catalyst as that used in the present work, we have shown that the Mo^{VI} cations in isolated molybdate species are fully reduced in H_2 to Mo^{IV} cations.[28] Thus, the shift in Mo K-edge energy from 8.1 to 5.0 eV and the reduction in the integrated intensity of the pre-edge feature from 2.2 to 0.96 eV are indicative of the complete reduction of Mo^{VI} to Mo^{IV}. Viewed in this light, the degree of Mo^{VI} reduction increases in the order $CH_4/O_2 \approx CH_4 \approx CO < CH_2O < H_2$ based on the results presented in Figure 1 and Table 1. The higher effectiveness of CH_2O as a reducing agent compared to CO is very likely due to the formation of H_2 when CH_2O decomposes under nonoxidizing conditions over MoO_x/SiO_2.[1] The absence of a large shift in the Mo K-edge energy when the catalyst is exposed to a mixture of 90% CH_4/10% O_2 suggests that virtually all of the Mo remains as Mo^{VI} during the oxidation of methane.

In-situ EXAFS data of MoO_x/SiO_2 gathered during exposure to flowing reductants at 873 K yielded results that were qualitatively similar to those obtained from XANES data. The magnitude of the Fourier transform of the k^3-weighted scattering function, $\chi(k)$, is presented in Figure 2 for MoO_x/SiO_2. The spectrum of calcined MoO_x/SiO_2 recorded under vacuum at 77 K is shown for comparison to the spectrum gathered in-situ under flowing 10% O_2/He at 873 K. The spectra are qualitatively identical, and only a slight reduction in spectral intensity is observed at 873 K relative to the intensity observed at 77 K.

While an effort was made to fit the EXAFS spectra using standard techniques, it was not possible to determine a unique set of EXAFS parameters because of strong correlations between these parameters arising from both overlap of the oxygen scatterers at low R values with contributions from atomic EXAFS[42] and the uncertainty in the Debye−Waller factors of the oxygen shells of MoO_x/SiO_2. These difficulties are likely responsible for the conflicting findings reported previously for MoO_x/SiO_2.[13,14] Nevertheless, the EXAFS data could still be used in a qualitative manner in order to assess the extent of

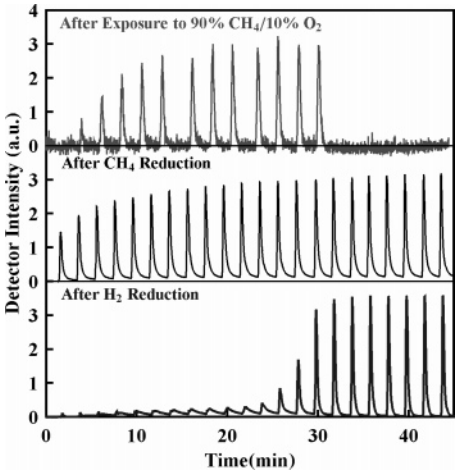

Figure 3. O_2 pulse chemisorption spectra for MoO_x/SiO_2 treated in flowing H_2, CH_4, and 90% CH_4/10% O_2 at 873 K. O_2 chemisorption was conducted at 873 K with 1.79 μmol pulses of O_2 for samples treated in H_2 and CH_4 and with 17.4 nmol pulses of O_2 for the sample treated in 90% CH_4/10% O_2. The time axis expanded three times for the sample treated in 90% CH_4/10% O_2.

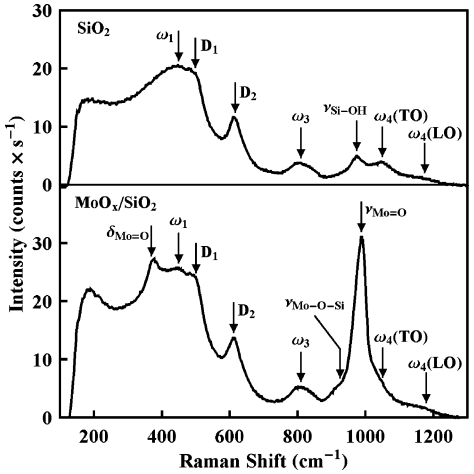

Figure 4. Raman spectra of bare SiO_2 and of MoO_x/SiO_2 recorded at 920 K under flowing air Raman bands. Bands are shown for SiO_2 (ω_1, ω_3, ω_4(TO), ω_4(LO), D_1, D_2, and ν_{Si-OH}) and SiO_2-supported MoO_x ($\delta_{Mo=O}$, $\nu_{Mo-O-Si}$, and $\nu_{Mo=O}$).

molybdate reduction. Under 10% O_2/He, oxygen backscattering peaks were observed in the Fourier transformed $k^3\chi(k)$ spectrum at 0.75, 1.20, and 1.60 Å. Under pure CH_4 and 4% CO/He, these peaks retained their shape but were decreased in intensity by ~15%. Under 1% CH_2O/He, the intensity of the peaks was reduced by ~35% and the peaks at 0.75 and 1.20 Å became poorly resolved. Under H_2, the peak intensity was ~50% of the observed intensity under 10% O_2/He. These results demonstrate a successively decreasing amount of oxygen coordinated to Mo during the reduction of MoO_x/SiO_2 which follows the order $CH_4 \approx CO < CH_2O < H_2$, consistent with the levels of reduction observed by XANES.

The reoxidation of MoO_x/SiO_2 reduced in pure H_2 and CH_4 was investigated by pulsed chemisorption of O_2, and the results are shown in Figure 3. The pulsed chemisorption spectrum of MoO_x/SiO_2 treated in 90% CH_4/10% O_2 is also shown in Figure 3 and will be discussed later. After reduction in pure H_2 at 873 K, MoO_x/SiO_2 takes up 1 O per Mo during titration with O_2 and therefore Mo^{IV} is the stable form of H_2-reduced MoO_x/SiO_2, as noted above.[28,30] The character of the titration curve following CH_4 reduction differs from that observed following H_2 reduction. After H_2 reduction, the chemisorption of O_2 by the reduced surface was very rapid. Each pulse of O_2 was almost entirely adsorbed by the catalyst until the catalyst approached saturation (~1 O per Mo), after which the breakthrough of O_2 occurred rapidly, and all of the O_2 in each pulse passed through the oxygen-saturated catalyst bed. By contrast, the consumption of O_2 by the CH_4-reduced catalyst was slow. CH_4-reduced MoO_x/SiO_2 did not take up entire O_2 pulses but consumed part of each pulse for many pulses. There was no sharp breakthrough of O_2 to indicate that the surface had been saturated with oxygen. After 45 pulses, the sample had consumed 0.55 O per Mo and was still consuming O slowly with each pulse.

In-situ Raman spectroscopy was used to characterize the MoO_x/SiO_2 in its fully oxidized state and after reduction in pure CH_4. The Raman bands of SiO_2 and of SiO_2-supported MoO_x are identified in Figure 4 based on previously published work for MoO_x/SiO_2 under flowing air at 920 K.[13,19,32,33] The SiO_2 features ω_1, D_1, D_2, ω_3, ν_{Si-OH}, ω_4(TO), and ω_4(LO) were observed at 450, 500, 614, 810, 975, 1051, and 1179 cm^{-1}, respectively. The Mo═O bending and stretching modes $\delta_{Mo=O}$ and $\nu_{Mo=O}$ were observed at 369 and 988 cm^{-1}, respectively.

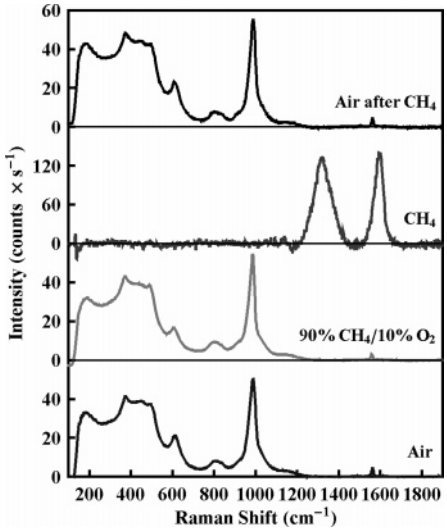

Figure 5. Baseline-subtracted Raman spectra of MoO_x/SiO_2 recorded at 920 K under flowing air, 90% CH_4/10% O_2, pure CH_4, and air after CH_4 treatment.

The shoulder observed at 925 cm^{-1} was the only feature that had not been previously assigned and is tentatively assigned to a stretching mode of Mo−O−Si bonds based on previous observations made by FTIR absorption spectroscopy.[43,44]

Figure 5 shows the Raman spectra of MoO_x/SiO_2 recorded at 920 K in air, in a mixture of 90% CH_4/10% O_2, and in pure CH_4. The Raman spectrum of MoO_x/SiO_2 recorded during CH_4 oxidation is indistinguishable from that observed under flowing air, in agreement with a previous report.[18] However, none of the Raman bands of MoO_x/SiO_2 are observed during treatment under pure CH_4 at 920 K. Instead, an intense fluorescent background centered at about 1450 cm^{-1} is observed together with two peaks at 1390 and 1560 cm^{-1}, which are attributable to amorphous carbon.[45−47] The deposition of carbon is consistent with the observation that the catalyst changes color from white to dark gray upon reduction in CH_4. The carbonaceous deposit is removed by exposure to flowing air for several minutes, after which the amorphous carbon peaks and intense fluorescent background disappear, and the Raman spectrum of MoO_x/SiO_2 is restored, as is shown in Figure 5. Hence, CH_4 reduction of MoO_x/SiO_2 deposits amorphous carbon on the surface, and during O_2 chemisorption by CH_4-reduced MoO_x/SiO_2, O_2 reacts

TABLE 2: Amount of O Adsorbed during O_2 Pulse Chemisorption by MoO_x/SiO_2 Treated at 873 K under CH_4/O_2 Mixtures of Varying CH_4 and O_2 Concentration

CH_4 Feed Fraction (%)	O_2 Feed Fraction (%)	O adsorbed (nmol O/g cat)	O adsorbed ($O/10^6$ Mo)
20	10	0	0 (53[a])
43	10	34	110
67	10	57	180
90	10	110	340
90	6.7	180	580

[a] Determined from the extrapolation of data obtained at higher CH_4 feed fractions.

with the amorphous carbon, rather than with reduced Mo centers. On the basis of the XAS results, it appears that CH_4 reduction of MoO_x/SiO_2 reduces the surface by much less than 2 e^- per Mo, and therefore, amorphous carbon is deposited onto MoO_x sites that remain nearly fully oxidized. The small amount of reduction observed by XAS during exposure to CH_4 may result from reduction of MoO_x by H_2 produced during carbon deposition. Apparently, H_2 reduction of the MoO_x does not proceed once the MoO_x are carburized, since the level of reduction was stabilized at $\ll 2$ e^- per Mo. Carbon deposition was not observed during CH_4 oxidation, as can be seen by comparison of the Raman spectra presented in Figure 5. This indicates that carbon deposition is much slower than carbon removal by O_2, so that during steady-state CH_4 oxidation carbon deposits do not accumulate on the catalyst.

The low level of reducibility of MoO_x by CH_4 implies that CH_4 oxidation over MoO_x/SiO_2 cannot proceed according to a Mars−van Krevelen mechanism in which stable surface O^{2-} anions are removed by CH_4 to yield products. For such a mechanism to produce CH_2O and H_2O, the surface would have to be reduced by 4 e^- per CH_4 converted, namely

$$CH_4 + 2O^{2-} \rightarrow CH_2O + H_2O + 4e^-$$

Since the MoO_x are isolated on SiO_2, such a mechanism would result in the reduction of Mo^{VI} to Mo^{II}. If, instead, a mechanism involving the removal of O^{2-} anions from two MoO_x sites was postulated, as has been done in the formulation of microkinetic models for CH_4 oxidation over MoO_x/SiO_2,[1,9] then it would be expected that the reduction of Mo^{VI} to Mo^{IV} would be observed under CH_4. Since the average reduction of Mo observed by XAS under CH_4 at 873 K is $\ll 2$ e^- per Mo, it is inferred that CH_4 is incapable of reducing MoO_x/SiO_2 by removing O^{2-} anions.

O_2 chemisorption was performed on MoO_x/SiO_2 after the catalyst was treated under CH_4/O_2 mixtures at 873 K in order to gage the level of catalyst reduction during steady-state CH_4 oxidation. The O_2-pulsed titration curve obtained after treatment of MoO_x/SiO_2 under 90% CH_4/10% O_2 is shown in Figure 3 for comparison to those obtained after H_2 and CH_4 treatment. The character of the O_2 pulsed titration curves obtained after treatment under CH_4/O_2 mixtures was similar to that obtained after treatment under H_2; the sample adsorbed O_2 rapidly until it was saturated, after which adsorption ceased. The level of reduction observed during CH_4 oxidation was very small, and pulses containing only 17.4 nmol O_2 were utilized to titrate the reduced sites of ~500 mg of MoO_x/SiO_2 after exposure to CH_4 oxidation conditions. The amounts of reduced sites titrated after treatments at 873 K under feeds of various CH_4/O_2 compositions are summarized in Table 2 as the number of O atoms adsorbed per Mo atom. As the CH_4 feed fraction was increased, the level of reduction of the surface increased. O_2 adsorption was measurable for CH_4 feed fractions $\geq$43%. After treatment under 90% CH_4/10% O_2, 340 O atoms were adsorbed per million Mo atoms. The level of reduction could also be increased by decreasing the O_2 feed fraction. After treatment under 90% CH_4/6.7% O_2, 580 O atoms were adsorbed per million Mo atoms. When a mixture of 20% CH_4/10% O_2 was used, no measurable adsorption of O_2 was observed. The amount of adsorption expected based on extrapolation of data gathered under CH_4/O_2 mixtures containing 43−90% CH_4 was 53 O atoms per million Mo atoms, which was near the detection limit of the technique. This is in good agreement with the previously reported amount of O_2 adsorption following treatment of MoO_x/SiO_2 with a loading of 2.67 wt % Mo at 873 K under 20% CH_4/10% O_2, which was reported as 13 nmol O/g of catalyst or 48 O atoms per million Mo atoms.[48]

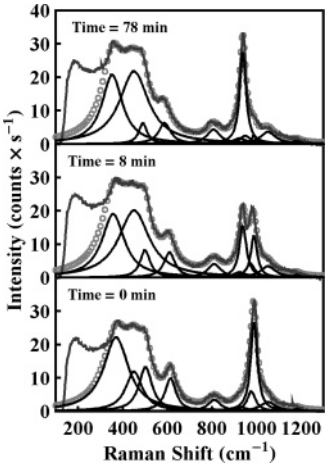

Figure 6. Baseline-subtracted Raman spectrum of MoO_x/SiO_2 recorded at 920 K after calcination in air and after 8 and 78 min under 40% CH_4/6% $^{18}O_2$/54% He. Open circles are the fit composed of the Lorentzian components shown on the abscissa. The total gas flow rate was 20 cm^3(STP)/min; the catalyst mass was 31.0 mg.

Isotopic Exchange of Oxygen during CH_4 Oxidation by $^{18}O_2$. Previous studies of CH_4 oxidation over SiO_2-supported oxides have determined that a large amount of the ^{16}O of SiO_2 is incorporated into the reaction products when a $CH_4/^{18}O_2$ mixture is used as the feed and reaction products are analyzed by mass spectrometry.[22,23] We have observed a similar phenomenon when a $H_2/^{18}O_2$ mixture is reacted over MoO_x/SiO_2.[28] Moreover, in-situ Raman spectroscopy revealed that ^{18}O is incorporated into the exposed surface of SiO_2. These studies revealed that the isotopic compositions of Mo═O species and H_2O were in quasi-equilibrium and that H_2O exchanged O atoms rapidly with the SiO_2 support. A similar approach was used in the present study in order to investigate the distribution of O isotopes between the products and the catalyst when CH_4 was oxidized by $^{18}O_2$ over MoO_x/SiO_2.

The Raman spectrum of MoO_x/SiO_2 is shown in Figure 6 after calcination at 920 K and after 8 and 78 min of exposure to a mixture containing 40% CH_4/6% $^{18}O_2$/54% He. As the oxidation of CH_4 proceeded, the intensity of the Mo═^{16}O band at 988 cm^{-1} decreased and the intensity of the Mo═^{18}O band at 938 cm^{-1} increased. After 78 min on stream, <10% of the oxygen in the Mo═O was ^{16}O. The substitution of ^{18}O by ^{16}O in Mo═O bonds was accompanied by a simultaneous red shift in the D_2 feature, associated with the surface of SiO_2.[32,34,36,37] After calcination, the position of the D_2 feature was observed at 614 cm^{-1}. After 78 min of exposure to the mixture of CH_4 and $^{18}O_2$, the frequency for this feature shifted to 588 cm^{-1},

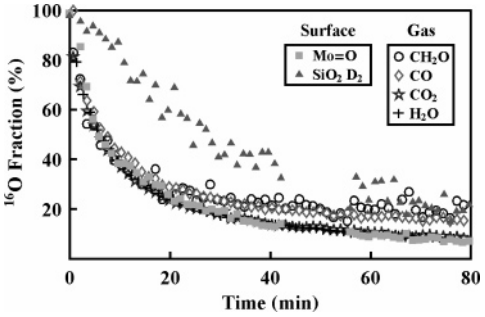

Figure 7. Isotopic composition of oxygen in surface Mo═O and SiO_2 D_2 features and in oxygenated reaction products vs time on stream during the reaction of 40% CH_4/6% $18O_2$/54% He at 920 K over MoO_x/SiO_2. The total gas flow rate was 20 cm^3(STP)/min; the catalyst mass was 31.0 mg.

indicating that 79% of the ^{16}O in the D_2 feature had been replaced by ^{18}O.

Figure 7 shows the isotopic compositions of the surface Mo═O and SiO_2 D_2 features as functions of time during exposure of the catalyst to a mixture of 40% CH_4/6% $^{18}O_2$/54% He at 920 K. The isotopic compositions of the oxygen-containing products are also shown in this figure. The isotopic compositions of H_2O and CO_2 are identical to that of the Mo═O feature at all times. We have recently shown that the exchange of oxygen between H_2O and Mo═O occurs very rapidly,[28] and previous work has demonstrated the rapid exchange of oxygen between CO_2 and MoO_x/SiO_2.[22] The ^{16}O fraction of the D_2 feature of SiO_2 decreases with time on stream but is significantly greater than that of the Mo═O feature at all times, indicating that ^{16}O is exchanged more slowly with the SiO_2 surface than with the supported MoO_x species. The ^{16}O fractions of CH_2O and CO are slightly greater than that of the Mo═O feature for reaction times >20 min but are less than that of the D_2 feature of SiO_2. The ^{16}O fraction of CH_2O approaches 20% after 80 min of reaction, whereas that of Mo═O is <10%. This is probably the result of direct oxygen exchange between CH_2O and the SiO_2 surface, which is enriched in ^{16}O relative to the MoO_x at any time on stream. CO is formed via decomposition of CH_2O over MoO_x/SiO_2,[1,2] and it has been shown previously that CO does not exchange oxygen at a significant rate with MoO_x/SiO_2.[22] As a consequence, the isotopic compositions of CH_2O and CO are expected to be identical, which is what was observed.

The amount of ^{16}O incorporated into oxygenated products was estimated by integration of the molar flow rates of ^{16}O-containing products over the duration of an experiment. Because the rate constants for exchange of oxygen between the products and the surfaces of the in-situ Raman cell were unknown, there was some uncertainty in the estimate but the amount of exchangeable oxygen was estimated as 22−30 O atoms per Mo atom. This is much more oxygen than the 5 O atoms coordinated to the supported MoO_x moieties and is about equal to the amount of oxygen on the surface of MoO_x/SiO_2.[28] Hence, in addition to the oxygen associated with the supported MoO_x moieties, all of the oxygen present on the surface of the SiO_2 support can be incorporated into the reaction products during CH_4 oxidation.

An effort was made to ascertain whether oxygen from the SiO_2 surface is incorporated into the reaction products as a direct consequence of the oxidation of CH_4 or as the result of the secondary exchange of oxygen between H_2O (or other oxygen-containing products) and the SiO_2 surface. To this end, a comparison was made between the kinetics of oxygen exchange between the gas phase and the D_2 feature of SiO_2 observed

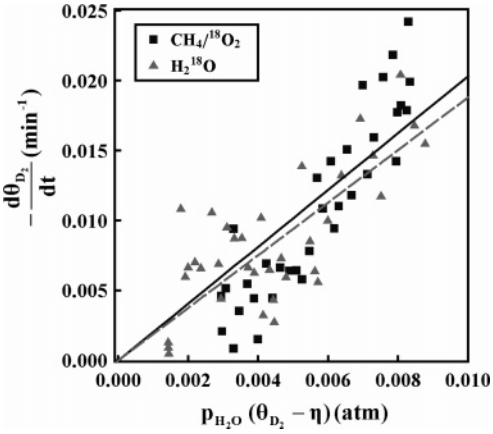

Figure 8. Rate of change of the ^{16}O fraction of the SiO_2 D_2 feature vs the driving force $p_{H_2O}(\theta_{D_2} - \eta)$ during CH_4 oxidation by $^{18}O_2$ over MoO_x/SiO_2 and during the exchange of oxygen between $H_2{}^{18}O$ and MoO_x/SiO_2 at 920 K. The solid line is the linear fit of CH_4 oxidation data with a slope of 2.0 $(atm\ min)^{-1}$; the dashed line is the linear fit of oxygen exchange data with a slope of 1.9 $(atm\ min)^{-1}$. Derivative data were smoothed by taking moving averages over 10 samples.

during CH_4 oxidation by $^{18}O_2$ over MoO_x/SiO_2 and the kinetics observed during exposure of MoO_x/SiO_2 to $H_2{}^{18}O$. Assuming the gas phase in the Raman cell is completely backmixed, the rate of exchange of oxygen between the oxygen of a surface feature j and gaseous H_2O is given by

$$r_j = n_j \frac{d\theta_j}{dt} = k_j p_{H_2O}[\eta(1-\theta_j) - \theta_j(1-\eta)] = -k_j p_{H_2O}(\theta_j - \eta) n_j - \frac{d\theta_j}{dt} = k_j p_{H_2O}(\theta_j - \eta)$$

where r_j is the (negative) rate of ^{16}O accumulation in the surface feature j in mol min^{-1}, n_j is the total number of moles of oxygen in the surface feature j, θ_j is the fraction of the oxygen in surface feature j that is 16-labeled, k_j is the rate constant for oxygen exchange in units of $(atm\ min)^{-1}$, p_{H_2O} is the partial pressure of H_2O, η is the fraction of oxygen in H_2O that is 16-labeled, and t is time.

To isolate the kinetics of oxygen exchange with the D_2 feature of SiO_2, the rate of depletion of ^{16}O from the D_2 feature, $-d\theta_{D_2}/dt$, can be plotted parametrically against the kinetic group $p_{H_2O}(\theta_{D_2} - \eta)$ to yield the oxygen exchange rate constant k_{D_2}. Such a plot is shown in Figure 8 for oxygen exchange with the SiO_2 D_2 feature occurring during exposure of MoO_x/SiO_2 to $H_2{}^{18}O$ and during the reaction of 40% CH_4/6% $^{18}O_2$. While the data are quite noisy due to experimental error, it is clear that the rates of depletion of ^{16}O from the D_2 feature are comparable for the two processes. Linear regression of the data in Figure 8 gives values of k_{D_2} equal to 1.9 and 2.0 $(atm\ min)^{-1}$ for exposure of the catalyst to $H_2{}^{18}O$ and for CH_4 oxidation by $^{18}O_2$, respectively. The similarity in the values of k_{D_2} for the two processes indicates that the incorporation of ^{16}O into the products of CH_4 oxidation occurs after these products are formed rather than during the process of their formation. If the opposite were true, then the rate of oxygen exchange would have been greater during the reaction of CH_4 with $^{18}O_2$ than during the exposure of the catalyst to $H_2{}^{18}O$. This view is supported by the observation that the rate of exchange between $H_2{}^{18}O$ and the D_2 feature of SiO_2 was ~0.5 μmol min^{-1}, whereas the rate of oxygen consumption to produce products was ~20 μmol min^{-1}. Therefore, during CH_4 oxidation by $^{18}O_2$, the ^{16}O of the SiO_2 surface is exchanged into the gas phase primarily by direct

TABLE 3: Steady-State Activity and Selectivity of MoO_x/SiO_2 at 873 K vs CH_4 and H_2O Feed Fractions[a]

				product selectivity		
CH_4 feed fraction (%)	H_2O feed fraction (%)	CH_4 conversion (%)	CH_4 consumption rate (μmol CH_4/cm^3 cat × s)	CH_2O (%)	CO (%)	CO_2 (%)
21	0	2.8	0.44	48	38	14
20	0.68	4.4	0.69	42	46	11
21	1.0	5.0	0.77	41	48	10
20	2.0	4.9	0.75	40	49	10
78	0	2.0	1.2	45	44	11
78	2.0	3.3	2.0	40	52	8

[a] Feed includes 10% O_2, balance He. Total gas flow rate, 30 cm^3(STP)/min; catalyst mass, 196 mg; pressure, 2 psig; contact time, 0.15 s

exchange with $H_2{}^{18}O$ produced by the reaction. A small amount of direct exchange between CH_2O and the surface oxygen of SiO_2 probably also occurs, as evidenced by the slight enrichment in the ^{16}O fraction of CH_2O and CO relative to the ^{16}O fraction of Mo═O shown in Figure 7. Since the oxygen of the SiO_2 support is not involved in the redox cycles that convert CH_4 to oxygenated products, the redox processes that convert CH_4 to products involve only the O atoms present in the isolated MoO_x species.

Effect of H_2O Addition on the Rate of CH_4 Oxidation. The addition of H_2O to the feed during CH_4 oxidation over MoO_x/SiO_2 yields useful information regarding the reaction mechanism. The activity for methane conversion and the product distribution are tabulated in Table 3 vs feed fractions of CH_4 and H_2O at 873 K with the O_2 feed fraction fixed at 10% and the contact time fixed at 0.15 s. With no H_2O in the feed, the rate of CH_4 consumption increased from 0.44 to 1.2 μmol/(cm^3 cat s) as the feed fraction of CH_4 was increased from 20 to 78%. This indicates that the kinetics of CH_4 oxidation are less than first order with respect to CH_4, as we have recently reported.[1] As the H_2O feed fraction was increased from 0 to 1.0% with the CH_4 feed fraction fixed at 20% and the contact time fixed at 0.15 s, the rate of CH_4 consumption increased from 0.44 to 0.77 μmol/(cm^3 cat s). This large increase in CH_4 conversion was accompanied by slight decreases in CH_2O selectivity from 48 to 41% and in CO_2 selectivity from 14 to 10% and a slight increase in CO selectivity from 38 to 48%. Increasing the feed fraction of H_2O to 2.0% did not further enhance the rate of CH_4 oxidation or affect the product distribution. A similar trend has been reported for CH_4 oxidation by N_2O over MoO_x/SiO_2.[10] When the feed fraction of CH_4 was increased from 20 to 78%, the mole fraction of H_2O in the reactor effluent increased from ~0.9 to 2.3%, so it might be expected that the addition of H_2O to the 78% CH_4 feed would not enhance the CH_4 conversion. However, the addition of 2.0% H_2O to the 78% CH_4 feed did result in a large enhancement in the rate of CH_4 consumption from 1.2 to 2.0 μmol/(cm^3 cat s).

Summary of Observations and Discussion of Mechanism of CH_4 Oxidation. The XAS and in-situ Raman observations reported here indicate that isolated molybdate species supported on SiO_2 cannot be reduced significantly by CH_4 at 873 K. On the other hand, significant reduction of molybdate species occurs if H_2 is the reducing agent and a moderate degree of reduction is observed with CH_2O. In the latter case, H_2 produced via CH_2O decomposition is believed to be the actual reducing agent, since CO, the other decomposition product, is ineffective for the reduction of isolated molybdate species. Oxygen titration experiments indicate that only ~50−500 ppm of the molybdate species is reduced from Mo^{VI} to Mo^{IV} during steady-state CH_4 oxidation at 873 K. These findings suggest that the oxygen atoms involved in the oxidation of CH_4 to CH_2O are not those coordinated with the stable molybdate species but, rather, are present in metastable structures formed via the reaction of gas-phase O_2 with the molybdate species. This deduction is in agreement with that drawn from the previously reported observation that a pulse of CH_4 without O_2 is converted to CH_2O over MoO_x/SiO_2 to a much smaller extent than a pulse of CH_4 including O_2.[48]

SCHEME 1. Proposed Mechanism of CH_4 Oxidation at Isolated, SiO_2-supported MoO_x Sites

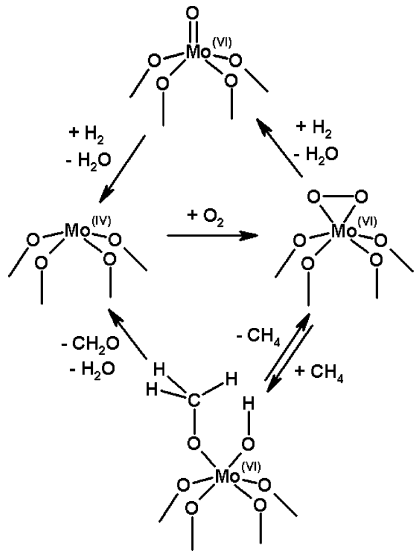

A mechanism that is consistent with the findings of the present work and with the findings of previous studies is shown in Scheme 1. The first step in the reaction network is a two-electron reduction of the isolated molybdate species by H_2, which is present in small concentration under steady-state conditions as a product of CH_2O decomposition.[1,49,50] The Mo^{IV} cations associated with the reduced molybdate species are then oxidized by O_2 to form peroxide species. The reaction of the molybdenum peroxide species with CH_4 produces CH_2O and H_2O. Alternatively, the peroxide can react with H_2 to regenerate the stable Mo^{VI}-containing molybdate species. The dissociative adsorption of CH_4 on the peroxide species is taken to be reversible and quasi-equilibrated. The rate-limiting step, leading to CH_2O and H_2O, is the abstraction of a proton from the methoxide species formed via CH_4 adsorption. The H_2 shown as the reducing agent for the oxidized molybdate species is envisioned to originate from the decomposition of CH_2O formed as the principal reaction product during steady-state CH_4 oxidation.[1]

Scheme 2 is an extension of Scheme 1, which is written with the aim of explaining the increase in the rate of methane oxidation with increasing H_2O partial pressure. Water is shown to hydrolyze Mo−O−Si bonds reversibly, and this reaction may be at quasi-equilibrium under reaction conditions, as suggested by isotopic labeling studies.[28] With increasing concentration in the gas phase, the concentration of surface hydroxide groups

SCHEME 2. Proposed Mechanism of CH_4 Oxidation at Isolated, SiO_2-supported MoO_x Sites, Including Parallel Pathways Enabled by the Presence of H_2O[a]

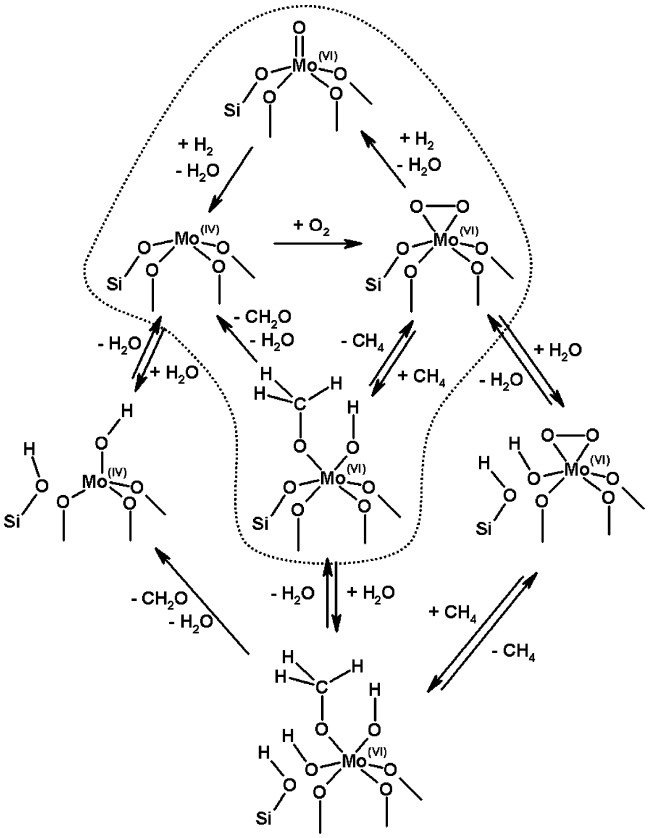

[a] The pathways outside of the dashed envelope are active when H_2O is present in the gas phase.

would increase, thereby enhancing their availability for reaction with the methoxide species produced during the activation of methane. It should be noted that excessive addition of H_2O to the feed would be detrimental, since complete hydrolysis of all Mo−O−Si bonds can lead to the removal of Mo from the support as volatile $MoO_2(OH)_2$. This phenomenon has been observed in our laboratory for MoO_x/SiO_2 catalysts with Mo loadings ranging from 0.2 to 9.3 Mo/nm^2.[51]

The large number of surface species and reaction pathways associated with the mechanism shown in Scheme 2 precludes quantitative fitting of the scheme to the observed kinetics. Nevertheless, this reaction mechanism is consistent with the observation of a lower than first-order rise in the rate of CH_4 oxidation with increasing CH_4 partial pressure.[1] Since the reaction of methoxide species with hydroxyl species is thought to be rate limiting, the surface concentration of methoxide species will increase with increasing CH_4 partial pressure, thereby shifting the equilibrium for the reversible adsorption of CH_4 to the right

$$CH_4 + Mo(OSi\equiv)_4(O_2) \rightleftarrows Mo(OSi\equiv)_4(OCH_3)(OH)$$

The increased surface concentration of methoxide drives the rate of the reverse reaction (methane desorption), so that the increase in methoxide concentration with respect to CH_4 is less than linear. Hence, the observed rate of CH_4 oxidation is less than first order with respect to CH_4 partial pressure. Unfortunately, the rates of reaction of the surface peroxide and surface methoxide are apparently too rapid to allow their concentrations to be quantified or even to allow their observation by in-situ Raman spectroscopy.

Scheme 1 is consistent with prior observations made in the literature. As noted above, it has been reported that a pulse of CH_4 without O_2 reacts over isolated Si-supported molybdate species to a much smaller extent than does a pulse of CH_4 including O_2.[48] The authors of this study attribute the difference in reactivity for the two cases to a metastable form of surface oxygen that is incompletely reduced, such as, for example, the Mo-bound peroxide species shown in Schemes 1 and 2. Such an active form of surface oxygen is also consistent with surface potential measurements of MoO_x/SiO_2 made previously during CH_4 oxidation. By measuring the change in surface potential under varying partial pressures of CH_4 and O_2, it was determined that the form of oxygen that is active for CH_4 oxidation is reduced by one electron per O atom.[52] The Mo-bound peroxide proposed in Schemes 1 and 2 is representative of such a species.

Previously published schemes for CH_4 oxidation, including ours, have attempted to explain the kinetics for CH_4 oxidation over MoO_x/SiO_2 by mechanisms in which multiple oxide anions react with CH_4 to yield CH_2O, H_2O, and a reduced catalyst.[1,9,10] While such mechanisms do describe CH_4 oxidation kinetics successfully,[1,9] they predict a much greater level of molybdate reduction (10−20%) than is observed experimentally.[1] The inability of CH_4 to reduce MoO_x/SiO_2 significantly, as observed here by XAS, is perhaps the strongest evidence that such mechanisms are incorrect physically. Such mechanisms have also relied on the participation of multiple Mo-containing sites, which is inconsistent with the fact that the highest specific activity for methane oxidation is observed for MoO_x/SiO_2 catalysts in which Mo is present as the sole isolated molybdate species. Such mechanisms are inconsistent, as well, with the findings that the active form of surface oxygen is short-lived[48] and reduced by one electron per O atom.[52] Hence, we believe that the mechanism shown in Schemes 1 and 2 is more likely to be physically correct than previously published mechanisms.

Some precedent does exist for the existence of Mo peroxides and for their activity for the oxidation of organic molecules. Peroxide-ligated Mo complexes have been observed by Raman spectroscopy both in solution and in crystalline solids[53,54] and are known to catalyze the oxidations of alcohols, amines, and sulfides at low temperatures.[55] Furthermore, metal peroxide species have been implicated as the active surface species responsible for the oxidation of CH_4 to CH_3OH over $Fe_{0.5}Al_{0.5}PO_4$ and have been observed by in-situ IR spectroscopy at 623 K.[56] Efforts undertaken in the course of the present study to observe peroxide species on MoO_x/SiO_2 by Raman spectroscopy under similar conditions were not successful, probably because of the much lower concentration of active metal in MoO_x/SiO_2 as compared to $Fe_{0.5}Al_{0.5}PO_4$. Nevertheless, the indirect evidence for peroxide species presented above support the conclusion that the formation of such species is an essential step in the oxidation of methane to formaldehyde.

Conclusions

MoO_x/SiO_2 prepared with a Mo loading of 0.44 Mo/nm^2 consists of isolated, pentacoordinated species containing a single Mo═O bond. These species are readily reduced by H_2 to molybdate species containing Mo^{IV} cations, but CH_4 and CO are not effective reducing agents for this process. During steady-state oxidation of CH_4 to CH_2O, only ∼50−500 ppm of Mo^{VI} in the catalyst is reduced to Mo^{IV}. On the basis of these observations, it is proposed that the active species for methane oxidation is a peroxide species formed by the reaction of O_2 with the low concentration of reduced molybdate species present on the catalyst surface. As shown in Schemes 1 and 2, the

activation of methane is envisioned to be reversible and at quasi-equilibrium. In this scheme, the rate-limiting step for the formation of CH_2O and H_2O is taken to be proton abstraction from methoxide groups formed by the dissociative adsorption of CH_4 by surface peroxide groups. Isotopic tracer experiments show that H_2O rapidly exchanges O atoms with the dispersed molybdate species and with the silica support. However, the oxygen of the silica support does not participate directly in the catalytic cycles that oxidize CH_4. The addition of low concentrations of H_2O to the feed enhances the rate of methane oxidation, and this phenomenon is ascribed to an enhancement in the concentration of surface hydroxide groups on the catalyst surface (see Scheme 2).

Acknowledgment. This work was supported by the Methane Conversion Cooperative sponsored by BP.

References and Notes

(1) Ohler, N.; Bell, A. T. *J. Catal.* **2005**, *231*, 115.
(2) Spencer, N. D.; Pereira, C. J. *AIChE J.* **1987**, *33*, 1808.
(3) Bañares, M. A.; Fierro, J. L. G. In *Catalytic Selective Oxidation*; Oyama, T., Hightower, J. W., Eds.; ACS Symposium Series 523; American Chemical Society: Washington, DC, 1993; p 354.
(4) Parmaliana, A.; Arena, F. *J. Catal.* **1997**, *167*, 57.
(5) Parmaliana, A.; Frusteri, F.; Mezzapica, A.; Scurrell, M. S.; Giordano, N. *J. Chem. Soc., Chem. Commun.* **1993**, 751.
(6) Arena, F.; Parmaliana, A. *Acc. Chem. Res.* **2003**, *36*, 867.
(7) Garibyan, T. A.; Margolis, L. Y. *Catal. Rev. − Sci. Eng.* **1989**, *31*, 355.
(8) Spencer, N. D.; Pereira, C. J.; Graselli, R. K. *J. Catal.* **1990**, *126*, 546.
(9) Amiridis, M. D.; Rekoske, J. E.; Dumesic, J. A.; Rudd, D. F.; Spencer, N. D.; Pereira, C. J. *AIChE J.* **1991**, *37*, 87.
(10) Liu, H.-F.; Liu, R.-S.; Liew, K. Y.; Johnson, R. E.; Lunsford, J. H. *J. Am. Chem. Soc.* **1991**, *37*, S **1984**, *106*, 4117.
(11) Roark, R. D.; Kohler, S. D.; Ekerdt, J. G. *Catal. Lett.* **1992**, *16*, 71.
(12) Roark, R. D.; Kohler, S. D.; Ekerdt, J. G.; Kim, D. S.; Wachs, I. E. *Catal. Lett.* **1992**, *16*, 77.
(13) de Boer, M.; van Dillen, A. J.; Koningsberger, D. C.; Geus, J. W.; Vuurman, M. A.; Wachs, I. E. *Catal. Lett.* **1991**, *11*, 227.
(14) Takenaka, S.; Tanaka, T.; Funabiki, T.; Yoshida, S. *J. Phys. Chem. B* **1998**, *102*, 2960.
(15) Bañares, M. A.; Hu, H.; Wachs, I. E. *J. Catal.* **1994**, *150*, 407.
(16) Hu, H.; Wachs, I. E.; Bare, S. R. *J. Phys. Chem.* **1995**, *99*, 10897.
(17) Faraldos, M.; Bañares, M. A.; Anderson, J. A.; Hu, H.; Wachs, I. E.; Fierro, J. L. G. *J. Catal.* **1996**, *160*, 214.
(18) Bañares, M. A.; Spencer, N. D.; Jones, M. D.; Wachs, I. E. *J. Catal.* **1994**, *146*, 204.
(19) Bañares, M. A.; Hu, H.; Wachs, I. E. *J. Catal.* **1995**, *155*, 249.
(20) Williams, C. C.; Ekerdt, J. G.; Jehng, J.-M.; Hardcastle, F. D.; Turek, A. M.; Wachs, I. E. *J. Phys. Chem.* **1991**, *95*, 8781.
(21) Mauti, R. S.; Mims, C. A. In *Methane and Alkane Conversion Chemistry*; Bhasin, M. M., Slocum, D. W., Eds.; Plenum Press: New York, 1995; p 137.
(22) Mauti, R.; Mims, C. A. *Catal. Lett.* **1993**, *21*, 201.
(23) Koranne, M. M.; Goodwin, J. G., Jr.; Marcelin, G. *J. Catal.* **1994**, *148*, 378.
(24) Pitchai, R.; Klier, K. *Catal. Rev. − Sci. Eng.* **1986**, *28*, 13.
(25) Khan, M. M.; Somorjai, G. A. *J. Catal.* **1985**, *91*, 263.
(26) Aoki, K.; Ohmae, M.; Nanba, T.; Takeishi, K.; Azuma, N.; Ueno, A.; Ohfune, H.; Hayashi, H.; Udagawa, Y. *Catal. Today* **1998**, *45*, 29.
(27) Spencer, N. D. *J. Catal.* **1988**, *109*, 187.
(28) Ohler, N.; Bell, A. T. *J. Phys. Chem. B* **2005**, *109*, 23419.
(29) Ravel, B.; Newville, M. *Phys. Scr., T* **2005**, *115*, 1007.
(30) Desikan, A. N.; Huang, L.; Oyama, S. T. *J. Phys. Chem.* **1991**, *95*, 10050.
(31) Su, S. C.; Carstens, J. N.; Bell, A. T. *J. Catal.* **1998**, *176*, 125.
(32) Galeener, F. L.; Mikkelsen, J. C., Jr. *Phys. Rev. B* **1981**, *23*, 5527.
(33) Mestl, G.; Srinivasan, T. K. K. *Catal. Rev. − Sci. Eng.* **1998**, *40*, 451.
(34) Galeener, F. L.; Geissberger, A. E. *Phys. Rev. B* **1983**, *27*, 6199.
(35) Uchino, T.; Tokuda, Y.; Yoko, T. *Phys. Rev. B* **1998**, *58*, 5322.
(36) Phillips, J. C. *Phys. Rev. B* **1986**, *33*, 4443.
(37) Phillips, J. C. *Phys. Rev. B* **1987**, *35*, 6409.
(38) Armour, A. W.; Drew, M. G. B.; Mitchell, P. C. H. *J. Chem. Soc., Dalton Trans.* **1975**, *14*, 1493.
(39) Busca, G. *J. Raman Spectrosc.* **2002**, *33*, 348.
(40) Cornac, M.; Janin, A.; Lavalley, J. C. *Polyhedron* **1986**, *5*, 183.
(41) Bañares, M. A.; Wachs, I. E. *J. Raman Spectrosc.* **2002**, *33*, 359.
(42) Rehr, J. J.; Booth, C. H.; Bridges, F.; Zabinsky, S. I. *Phys. Rev. B* **1994**, *49*, 12347.
(43) Seyedmonir, S. R.; Abdo, S.; Howe, R. F. *J. Phys. Chem.* **1982**, *86*, 1233.
(44) Cornac, M.; Janin, A.; Lavalley, J. C. *Infrared Phys.* **1984**, *24*, 143.
(45) Xiao, T.-C.; Wang, H.-T.; York, A. P. E.; Green, M. L. H. *Catal. Lett.* **2002**, *83*, 241.
(46) Bartlett, B. F.; Tysoe, W. T. *Catal. Lett.* **1997**, *46*, 101.
(47) Knight, D. S.; White, W. B. *J. Mater. Res.* **1989**, *4*, 385.
(48) Parmaliana, A.; Arena, F.; Sokolovskii, V.; Frusteri, F.; Giordano, N. *Catal. Today* **1996**, *28*, 363.
(49) Baldwin, T. R.; Burch, R.; Squire, G. D.; Tsang, S. C. *Appl. Catal.* **1991**, *74*, 137.
(50) Walker, J. F. *Formaldehyde*; ACS Monograph Series, 3rd ed.; Reinhold: New York, 1964.
(51) Ohler, N. Ph.D. Dissertation, University of California, Berkeley, CA, 2005.
(52) Barbaux, Y.; Elamrani, A.; Bonnelle, J. P. *Catal. Today* **1987**, *1*, 147.
(53) Arab, M.; Bougeard, D.; Aubry, J. M.; Marko, J.; Paul, J. F.; Payen, E. *J. Raman Spectrosc.* **2002**, *33*, 390.
(54) Dengel, A. C.; Griffith, W. P.; Powell, R. D.; Skapski, A. C. *J. Chem. Soc., Dalton Trans.* **1987**, 991.
(55) Maiti, S. W.; Abdul Malik, K. M.; Bhattacharyya, R. *Inorg. Chem. Commun.* **2004**, *7*, 823.
(56) Otsuka, K.; Wang, Y. *Appl. Catal. A* **2001**, *222*, 145.